Rare Metal Materials and Engineering
Volume 47, Issue 6, June 2018
Online English edition of the Chinese language journal

Available online at www.sciencedirect.com
ScienceDirect

Cite this article as: Rare Metal Materials and Engineering, 2018, 47(6): 1729-1733.

ARTICLE

Tungsten Surface Morphology Control and Its Thermal Fatigue Behavior Under Cyclic Heat Loading

Wang Liang, Wang Bo, Li Shudan, Tang Yunhui, Song Xuemei, Yan Hui

Beijing University of Technology, Beijing 100124, China

Abstract: Thermal fatigue behavior under various cyclic heat loading is an important concern for tungsten as armor material in fusion devices. Surface morphology controlling experiments have been performed on polycrystalline tungsten using an ECR plasma system and cyclic heat loading tests have been conducted upon the polished and modified samples using an electron beam apparatus. The results indicate that the surface topography has little effect on the characteristics of damage caused by the cycle plastic deformation during the cyclic heat loading. The micro-cracks and extrusions form in some grains after suffered 300 cyclic heat loading, which are aligned in different directions for varying grains. In addition, the modified specimens with both different triangular pyramid and homogeneous nanostructures were fabricated by dry etching under different conditions. The cross-section of damage regions were analyzed and a set of schematic diagram was presented to explain the mechanism for the formation of micro-cracks and extrusions under cyclic heat loading.

Key words: tungsten; surface morphology controlling; cyclic heat loading; thermal fatigue

Tungsten (W) will be used in the ITER divertor as a plasma facing material (PFM) and in many future fusion devices owing to its good thermal properties and low erosion rate[1,2]. Tungsten armor material will be exposed to extreme conditions of steady-state heat loading and several types of transient heat loading during operations[3]. Therefore, tungsten would suffer a variety of cyclic heat loading and the heat loading may lead to two kinds of damage of W materials: one is cracks, surface melting, evaporation, etc. caused by transient high heat flux (HHF) loads and the other is thermal fatigue phenomenon caused by stress with different strain rates under fluctuation of temperature, which results from unstable heat flux[4,5]. Recently, a series of HHF loads tests have been carried out on tungsten using either an electron beam or a pulsed laser apparatus. From these results, it is concluded that the damage types, such as roughening, cracks and surface melting, evolve as a function of transient heat loads, number of pulses and temperature of the W substrate[6-8]. However, few studies focus on the thermal fatigue caused by cyclic heat loading on the armor materials in fusion devices. As is known, the temperature fluctuations always exist in ITER and future fusion devices. So the thermal fatigue should be considered to a serious concern to the performance of W-PFMs.

In this paper, different nanostructures have been fabricated on the surface of tungsten substrates by dry etching under df ferent conditions to study the impacts of different surface morphologies on fatigue property under cyclic heat loading. The electron beam apparatus, used to generate cyclic heat loads, has been employed to investigate the thermal fatigue behavior of tungsten substrates. The central maximum heat flux is 48 MW/m^2 with the pulse duration of 1 s through the cyclic heat loading.

1 Experiment

Material used in the present work was recrystallized tungsten with a high purity (>99.9%), purchased from AT&M Refractory Metal & Ceramics Branch (China). The test samples were cut to 10 mm×10 mm×2 mm pieces by wire-electro discharge. The surface of the samples was

Received date: June 17, 2017
Foundation item: National Magnetic Confinement Fusion Science Program of China (2013GB109003); National Natural Science Foundation of China (51571003)
Corresponding author: Wang Bo, Ph. D., Professor, School of Materials Science and Engineering, Beijing University of Technology, Beijing 100124, P. R. China, Tel: 0086-10-67396274, E-mail: wangbo@bjut.edu.cn

electro-chemically polished to a mirror-like finish with an arithmetic mean roughness (R_a) of less than 0.1 μm in order to obtain a well-defined reference surface. After polished, the substrates were ultrasonically cleaned in ethanol and deionized (DI) water and subsequently dried with nitrogen (N_2) gas.

The cleaned tungsten substrates were used to fabricate the nanostructures on the surface of the samples via two kinds of processes. A schematic of processing steps are shown in Fig.1, which shows deposition of thin film of nickel (Ni) on the tungsten substrates, followed by rapid thermal annealing to break the Ni film into nanoparticles. During the process, the nanoparticles were formed by themselves, thus having an advantage of relatively simple and cost-effective process. These Ni nanoparticles were used as an etch mask to pattern the tungsten substrates. Another process had the same dry etching parameters without the deposition of Ni and thermal annealing steps. According to the comparative study of the two methods, we investigated the effect of the Ni nanoparticles on the morphology of tungsten substrates.

To form the nanosized etch mask patterns, the Ni thin film was deposited on the samples by a magnetron sputtering system. The depositions were performed at a base pressure of 10~4 Pa, room temperature, 15 W of the power and 20 standard cubic centimeters (cm^3/min) of pure Ar. The target-substrate distance was 8 cm, the working pressure was 7 Pa and the deposition time was 10 and 25 min. The samples (with the nickel film) were annealed at 650 °C for 10 min under Ar protective environment.

Dry etching of the samples was carried out in an electron cyclotron resonance (ECR) plasma system with gas mixture of CF_4 (8 cm^3/min) and O_2 (5 cm^3/min). In the process of plasma etching, the working pressure was of 0.2 Pa. After the dry etching, the remaining Ni nanoparticles were removed by nitric acid rinse.

The thermal fatigue experiments were conducted upon the polished type A sample and the modified type B samples in the electron beam apparatus with 8 kV rated voltage. The polished and the modified specimens were mounted on a carbon crucible placed on a water-cooled Cu block. The thermal fatigue tests were conducted out with 300 pulsers at an absorbed power density of 48 MW/m^2 with a duration of 1 s followed by a 11 s interval to cool the loaded area to the base temperature.

The surface morphology of the substrates was observed by an S-4800 scanning electron microscope (SEM) using a field emission microscope with an operating voltage of 15 kV. The subsurface cross-section information after cyclic heat loading tests was obtained by focused ion beam (FIB) technology and imaging (SEM). In addition to SEM, electron backscatter diffraction (EBSD) was used to correlate the crystallographic orientation of grains to the surface morphology induced via cyclic heat loading.

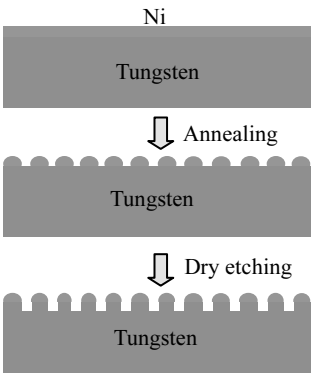

Fig.1 Schematic of the nanostructure fabrication process: depositing Ni film on tungsten substrate, thermal annealing and dry etching

2 Results and Discussion

2.1 Characteristics of nanostructure

The tilted-view SEM images in Fig.2 show different grain surface morphology of polycrystalline tungsten substrates modified by ECR plasma etching for 60 min. Owing to the anisotropic etching of polycrystalline tungsten, the whole tungsten surface is covered with triangular pyramid nanostructures with different orientations that are strongly affected by crystallographic orientation of the grains. Based on this fact, grain orientations could be determined using etch patterns[9]. It is similar to the way of preparation of pyramid structure on the silicon surface by anisotropic etching in NaOH solution. Unlike monocrystal silicon, the grains of tungsten substrates have different orientations, so the triangular pyramid nanostructures are various, as shown in Fig.2.

Fig.3 shows the tilted-view SEM images of morphologies of the nanostructures on tungsten substrates fabricated by ECR plasma etching for 60 min with different deposited time

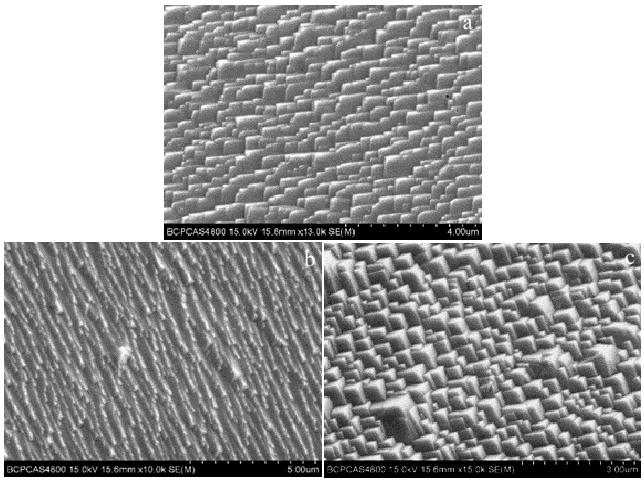

Fig.2 SEM images (23°-tilted oblique view) of the surface morphologies modified by ECR plasma etching, which represent three grains of different crystal orientations (a, b and c) in one tungsten sample

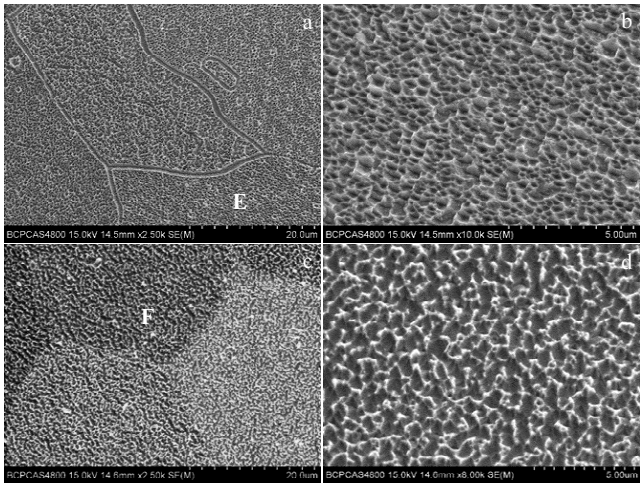

Fig.3 SEM images (23°-tilted oblique view) of surface morphologies of tungsten substrates modified by ECR plasma etching with different deposited time of Ni assisting: (a) 10 min, (c) 25 min, (b, d) is higher magnification of grains E and F shown in Fig.3a and Fig.3c, respectively

of Ni film assisting (10 min and 25 min). In these images, residual nickel nanoparticles have been removed by nitric acid rinse, and only tungsten nanostructures created out of the tungsten substrates are imaged. The images in Fig.3 show that the nanostructures fabricated on the tungsten surface are very uniform and not affected by the crystallographic orientation of the grains, especially with thicker Ni film assisting. Clearly, very different structures form by dry etching with Ni mask patterns. The images in Fig.3b and 3d illustrate that the characterization of the nanostructures fabricated is strongly affected by the thickness of Ni films. The average period between adjacent nanostructures becomes larger and the average diameter of nanostructures increases when the Ni film thickness increases. Compared with the images in Fig.2 and Fig.3, we can assume that the thermally annealed Ni nanoparticles play a decisive role in controlling the final characterization of the nanostructures on tungsten substrates.

The reason for the formation of the uniform nanostructures is the existence of Ni nanoparticles uniformly distributed over the tungsten surface obtained by thermal annealing process. This process occurs because the surface energy of the Ni film is larger than that of the interface and the underlying substrate when thermally heated, so the metal film collect into nanoparticles on the substrate surface to minimize its energy, like the mechanism of Ostwald ripening[10,11]. These Ni nanoparticles are used as etch mask patterns in the process of ECR plasma etching. Meanwhile, CF_4 and O_2 plasma are responsible for the etching of exposed tungsten substrates. With the etching process, the nickel mask also gets etched slowly, resulting in the uneven etching of the tungsten surface. In the end, the island-like nanostructures are formed onto the tungsten substrates. So the critical factor for fabricating the uniform nanostructures is the formation of large-scale nanosized etch mask patterns.

2.2 Thermal fatigue behavior

Finally, cyclic heat loading tests were conducted upon the polished type A and modified type B samples, with the transient heat flux loads at 48 MW/m^2. Fig.4 presents SEM images of the surface morphologies of type A and type B samples, which were exposed by 300 cyclic heat loading. In the case of the experiment, the cyclic heat loading rapidly increases and reaches about 48 MW/m^2 for 1 s as the electron beam irradiation starts. Subsequently, the heat loading rapidly decreases to zero and remains for 11 s. At the same time, the surface temperature of tungsten samples orders periodically alter with the change of heat loading.

For type A sample, micro-cracks and extrusions are observed on the surface with the cyclic heat loading, as shown in Fig.4a and 4b. In addition, micro-cracks along the grain boundaries form, where the bonding energy is weaker than that of other places. The directions of micro-cracks and extrusions differ from one grain to another, depending on the crystallographic orientation of the grains. The characteristics of the surface morphologies are similar to the results obtained in Ref. [12]. The author discussed that the morphologies are considered to be due to the repetitive anisotropic deformation and thermal fatigue by cyclic heat loading. However, the formation of the morphologies is not clearly explained.

The samples of type B have been fabricated with nanostructures on the surface before the cyclic heat loading tests. As the SEM images shown in Fig.4c and 4d, the characteristics of the surface morphologies, such as micro-cracks and extrusions, are similar to the results obtained on type A sample surface. Through the comparison between type A and type B, the surface morphology has little effect on the characteristics of micro-cracks and extrusions. The lines of micro-cracks vary from one grain to another, which reflects the close relationship between the morphology and crystallographic orientation of the grains. The formation of these directional micro-cracks and extrusions on surface might be caused by the shear or deformation along a certain slip plane of grain. In addition, the nanostructures fabricated by dry etching have deformed seriously after exposed by 300 cyclic heat loading shots (Fig.4e and 4f). The deformation is mainly due to the partial melting of the nanostructures caused by temperature rise during cyclic heat loading.

2.3 Mechanism of formation

The morphology of extrusions was also obtained in Ref. [13], which was called scale-like structures. However, the formation of the scale-like structures was not clearly explained. In order to get a meaningful and precise explanation of the mechanism for formation, the FIB cross-section of the micro-cracks and extrusions on type A sample surfaces were examined and depicted in Fig.5. Due to the effect of FIB

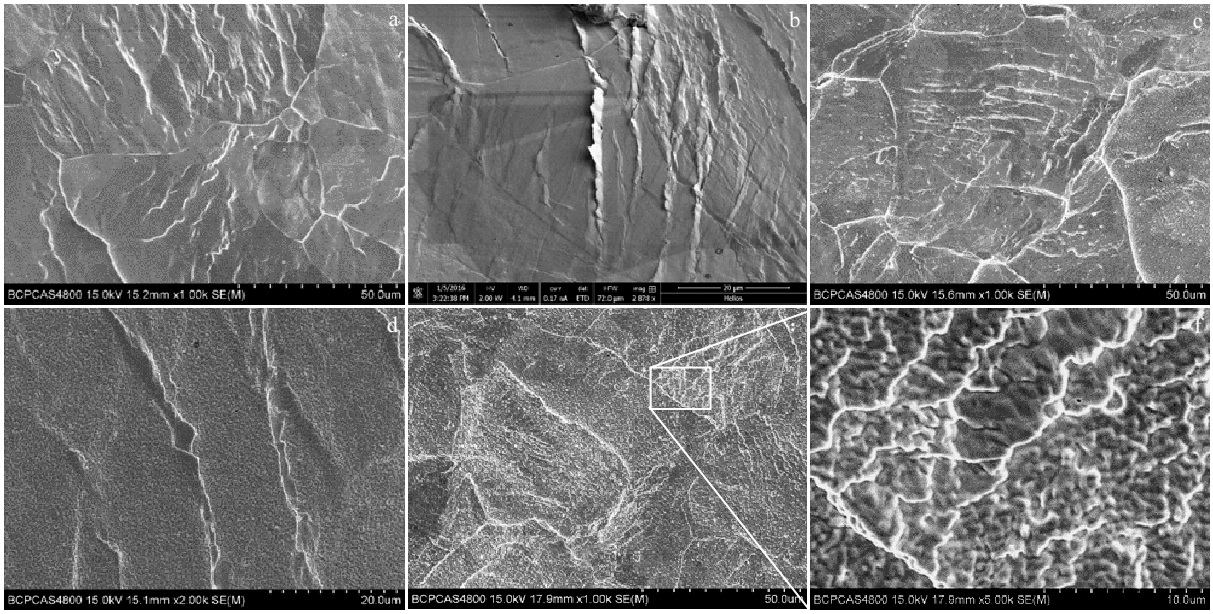

Fig.4 SEM images of surface morphologies after exposed to 300 cyclic heat loading: (a, b) different origins of type A sample; (c~e) different origins of type B sample; (f) higher magnification of square area in Fig.4e

processing, there is no useful information to ascertain the mechanism, as shown in Fig.5a and 5b. Therefore, the cross-section was treated by etching solution (0.5 g $K_3[Fe(CN)_6]$: 0.5 g NaOH:100 mL H_2O) for 20 min to eliminate the effects. After treatment, parallel lines arranged in a certain direction appear on the cross-section. The parallel lines correspond to the micro-cracks and extrusions on surface, and the lines of the two surfaces are connected to form a surface, which is a lattice plane. Based on the results above it can be stated that the micro-cracks and extrusions should be caused by the cycle plastic deformation, or in other words cyclic slip. The formation process of micro-cracks and extrusions could be explained by a schematic diagram in Fig.6[14]. During thermal fatigue tests, a cyclic switching-over of the process of heat loading and interval will subject the sample alternately to extrusion and tension stresses. As a consequence, cyclic stress

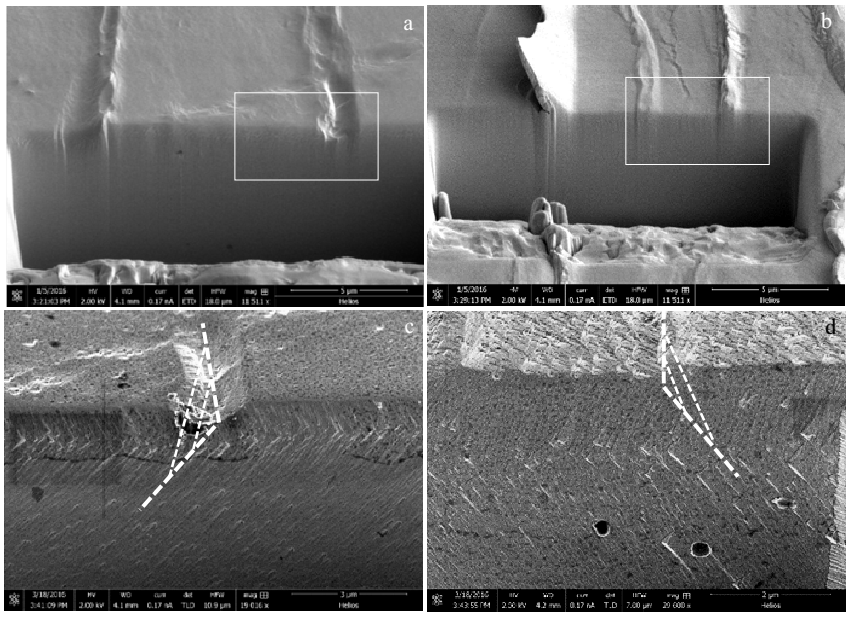

Fig.5 FIB cross-sectional SEM images of the different damage regions on type A sample after exposed to 300 cyclic heat loading: (a, b) original cross-section surface; (c, d) after etching

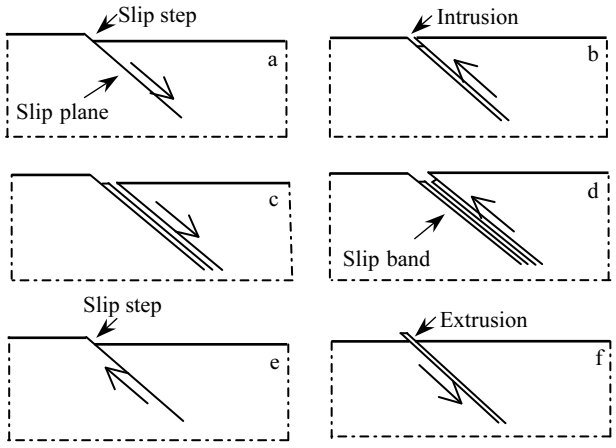

Fig.6 Schematic diagrams of the formation process of micro-cracks: (a, b) 1st cycle of cyclic slip; (c, d) 2nd cycle of cyclic slip; (e, f) extrusions

causes cyclic slip. As illustrated in Fig.6a, a slip step is created at the material surface when slip occurs in a grain. With the stress switching- over, reversed slip occurs in the same slip band. Since the slip is not a fully reversible process, reversed slip although occurring in the same slip band, will occur on adjacent parallel slip planes, as shown in Fig.6b. In the second cycle, the same sequence of events can occur (Fig.6c and 6d). As a result, a microscopical intrusion is created into the material, which in fact is a micro-crack. However, an extrusion would be obtained if the slip occurs at the left side of the slip band, as seen in Fig.6e and 6f.

In addition, micro-cracks and extrusions are only generated in some grains at the tungsten surface, because the shear stress on crystallographic slip planes differs from grain to grain, strongly depending on crystallographic orientation of the grains. In some grains, Schmidt factor (affected by crystallographic orientation) is relatively large and the slip system is most likely to occur.

3 Conclusions

1) The surface topography has little effect on the characteristics of damage caused by the cycle plastic deformation during the cyclic heat loading.

2) It is relevant to the distribution of shear stress on crystallographic slip planes of grain, which depend on the crystallographic orientation of the grains.

References

1 Philipps V. *Journal of Nuclear Materials*[J], 2011, 415(1): 2
2 Lemahieu N, Greuner H, Linke J *et al. Fusion Engineering and Design*[J], 2015, 98: 2020
3 Kotov V, Litnovsky A, Kukushkin A S *et al. Journal of Nuclear Materials*[J], 2009, 390: 528
4 Yuan Y, Greuner H, Böswirth B *et al. Journal of Nuclear Materials*[J], 2013, 438: 229
5 Loewenhoff T, Linke J, Pintsuk G *et al. Fusion Engineering and Design*[J], 2012, 87(7): 1201
6 Wirtz M, Bardin S, Huber A *et al. Nuclear Fusion*[J], 2015, 55(12): 123 017
7 Loewenhoff T, Bürger A, Linke J *et al. Physica Scripta*[J], 2011, T145: 14 057
8 Yu J H, Doerner R P, Dittmar T *et al. Physica Scripta*[J], 2014, T159: 14 036
9 Wang W H, Sun X, Köhlhoff G D *et al. Texture, Stress, and Microstructure*[J], 1995, 24(4): 199
10 Gentili D, Foschi G, Valle F *et al. Chemical Society Reviews*[J], 2012, 41(12): 4430
11 Lee J M, Kim B I. *Materials Science and Engineering A*[J], 2007, 449: 769
12 Tokunaga K, Kurishita H, Arakawa H *et al. Journal of Nuclear Materials*[J], 2013, 442(1): 297
13 Steudel I, Huber A, Kreter A *et al. Physica Scripta*[J], 2016, T167: 14 053
14 Schijve J. *Fatigue of Structures and Materials*[M]. Netherlands, Dordrecht: Kluwer Academic Publishers, 2001: 13

钨表面形貌控制及其在循环热载荷作用下的热疲劳性能

王 亮，王 波，李曙丹，汤云晖，宋雪梅，严 辉
(北京工业大学，北京 100124)

摘 要：钨作为聚变装置中的壁材料在各种循环热载荷作用下的热疲劳行为是一个重要的问题。采用电子回旋共振（ECR）等离子体系统在多晶钨表面进行形貌控制实验，然后采用电子束对抛光和具有一定表面形貌的样品开展循环热载荷实验。结果表明，表面形貌对在循环热载荷下发生的循环塑性变形造成的损伤特征影响很小，在 300 次循环热载荷下某些晶粒中形成了微裂纹及挤出片结构，它们在不同晶粒中按着某一特定的方向平行排列。此外，在不同条件下通过等离子体刻蚀在钨表面制备了不同的三棱锥状和均匀的纳米结构。对损伤区域的截面进行了分析并给出了在循环热载荷下这种结构形成过程的示意图。

关键词：钨；形貌控制；循环热载荷；热疲劳

作者简介：王 亮，男，1990 年生，硕士，北京工业大学材料科学与工程学院，北京 100124，电话：010-67396274，E-mail: 1072180735@qq.com